Available online at www.jrors.yazd.iau.ir

Journal Of Radar and Optical Remote Sensing and GIS

JRORS 3 (2022) 22–42

Investigation of the Relationship between Tectonic Morphological Indices and Seismic Acceleration in Indes, Aipak, Avaj and Kushk-e-Nusrat Fault Zones (Northwest of Saveh)

Bahar Rezaei Nahal[a], Mohsen PourKermani[b*], Mehdi Zare[c], Maryam Dehbozorgi[d], Reza Nozaem[e]

[a]*Department of Geology, North Branch, Islamic Azad University, Tehran, Iran*

[b]*Department of Geology, North Branch, Islamic Azad University, Tehran, Iran*

[c] *Professor, Department of International Institute of Earthquake Engineering and Seismology (IIEES), Tehran, Iran*

[d]*Department of Geology, Kharazmi University, Tehran, Iran*

[e]*School of Geology, College of Science, University of Tehran, Tehran, Iran*

Received 23 May 2022; Revised 4 July 2022; Accepted 20 July 2022

Abstract

The northwest zone of Saveh city is located in the Indes , Kooshk e Nosrat, Avaj and Ipak fault zones. Indes, Kooshk e Nosrat, Avaj and Ipak faults are considered as the major faults in central Iran, which are also active in the Quaternary and the their last movements are attributed to the present time, therefore, the estimation of morphometry in order to identify the effect of active tectonics on the tectonic evolution of drainage basins seems necessary. Therefore, in this study, six important morphotectonic indices were analyzed including longitudinal gradient of the river, asymmetry of drainage basin, hypsometric integral, Drainage basin shape, the ratio of the floor width to the valley height and mountain front. In order to model the formation of basins in the studied area, Arc Hydro software (Arc GIS add ins) has been used based on data derived from a digital elevation model. Then, 6 morphotectonic indices have been compiled and classified on each of the basins. Finally, the Active Tectonic Index (IAT) has been calculated, according to which the study area has been classified into 4 categories including very high, high, intermediate and low tectonic activity. According to the IAT index, 5% of the study area shows very high tectonic activity, 25% of the studied area has high tectonic activity, 65% of it has the average tectonic activity and about 5% of the tectonic activity are low. In this study, the highest level of tectonic activity can be seen in the north-eastern part of the area. In most sectors, the level of activity is high and intermediate, which is related to the activity of Kooshk-e-Nosrat, Aipak and Avaj faults.

Keywords: Active Tectonic, Morphometric Indice, Kooshk-e-Nosrat Fault, Indes Fault, Avaj Fault, Ipak Fault, Central Iran

[*] Corresponding author Tel: +98-9337827955.
Email address: baharrezaeinahal@yahoo.com

1. Introduction

Central Iran is a triangle region located in the center of Iran and is limited by the Alborz Highlands and a series of down holes and beltways of the direct faults of the Sanandaj-Sirjan Zone (Nabavi, 1976). In the whole Central Iran, especially in the marginal areas, the intensity of tectonic activities is high due to convergence between different zones (Alavi, 1991; Alavi, M., 1996) because of that, further fragmentation and more faults in the central Iran, as a continental margin, are expected. The study area is seismically active due to the presence of active faults such as; the Indes and Kooshk-e-Nosrat due to the continuity of the Arabic-Iranian convergence. So, in the map of Iran earthquake hazard zonation observed in high and very high-risk areas (Nowroozi and Mohajer-Ashjai, 1985) and the evidence of cut off and displacement of quaternary sediments by faults can confirmed that suggestion (Babaahmadi et al. 2010). The area can be accessed by the northwest of Saveh, southwest of the city of Karaj (Fig. 1a and b).

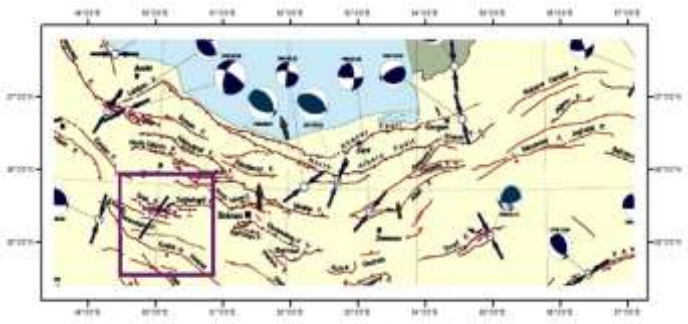

Figure 1a. Geolocation of the region (Hesami Azar et al.,2003)

Figure 1b. Access roads to the region (Hesami Azar et al.,2003)

This area is located in the part of Tabriz-Saveh tectonic zone (Alavi, 1991). Indes, Ipak, Avaj and Kooshk-e-Nosrat faults in the study area are among the main faults in the region, which are considered as active faults in the Quaternary according to seismic activity and other non-structural activities are observed and they are known as active faults in the Quaternary. To study the effect of recent activity of this fault zone, analysis of drainage basins located on the northwest of Saveh area has been used by morphometric indices. The morphometric characteristics of drainage basins have been extensively studied in many parts of the world (Altin and Altin, 2011; Reddy et al., 2004). Therefore, these indicators can be recognized and used as a useful tool in active tectonic reports (Keller and Pinter, 2002; Molin et al., 2004; Silvaet al., 2003). Also, the comparison between several morphotectonic indices with software such as Arc GIS can provide a precise numerical method for determining the tectonic activity of the area (Keller and Pinter, 1996). Therefore, for the active tectonics' estimation, the study area was extracted using ArcHydro plug-in ArcGIS software for drainage basins and river basins of each basin (Fig. 2). Six important tectonic indices have been investigated; longitudinal gradient of the river, asymmetry of drainage basin, hypsometric integrals, drainage basin shape ratio, the ratio of the width to the height of the valley and the index of the mountain forehead. In addition, field operations were performed to determine the accuracy of all indices and to observe fault related tectonic landforms and folds as well as to complete the results of this study, and the results were compared with morphotectonic analysis.

2. Methods

In order to determine the active tectonics in the drainage basin scale and using morphometric indices in the study area, first the drainage basins were extracted using the Arc Hydro plugin in Arc GIS 10.1 software and the area was divided into 40 separate basins. Then, the main river network was created in the study area and finally, morphometric indices were measured on the formed basins. To create a drainage network, first we fill the holes in the digitized raw height model, in fact, this hole or wells are defined by cells without a drainage path, and none of the surrounding cells is located below it. The result is a raster output with wells filled. In the next step, the drainage flow was calculated and a lattice outlet from each cell was created relative to its most progressive adjacent cell in the downward direction of the slope. Then, the accumulation of flow in different points of the digital height model is calculated and a raster output of the accumulated flow for each cell is obtained. Then this raster file is the accumulated flow change size, this size change is calculated by calculating logarithms based on 10 for all cells in a raster map. In this calculation, flow aggregation is used as input data. In the following, we create a flow grid and determine the flow class to know which category of drains are located. By doing this, a numerical value was obtained for each piece of line branch. To do this, there are two types of STRAHLER and SHREVE classifications that STRAHLER method is used in this study. In this method, the flow class only increases when other threads with the same category are disconnected.

Therefore, the connection of a first-order stream with a second-order stream, instead of creating a third-level connection, will remain a second-order stream. Finally, in order to extract the river network, the raster file has been converted to a linear network (Fig. 3). Consequently, by using the results of aforementioned steps, 40 drainage basins and their main rivers in the study area were defined by using the Arc GIS 10.1 software (Fig. 3).

Morphometric indices were measured by using digital elevation model and topographic maps that derived from it. In the next step, using 1: 100,000 geological map of the area the geological units and the main faults has been determined and in order to determine the activity of the structural elements in the area in quaternary units such as cones, the IRS P5 satellite image of the Army Geographic Organization has been used. Then the accuracy of the above results has been verified by conducting extensive field studies in all parts of the study area. Finally, the relationship between the quantitative morphometric data measured by the software, the structures obtained from field studies and the lines determined by satellite images in the study area has been analyzed and from their combination, the final index of active tectonic (IAT) has been determined and the relative active land development has been determined throughout the study area.

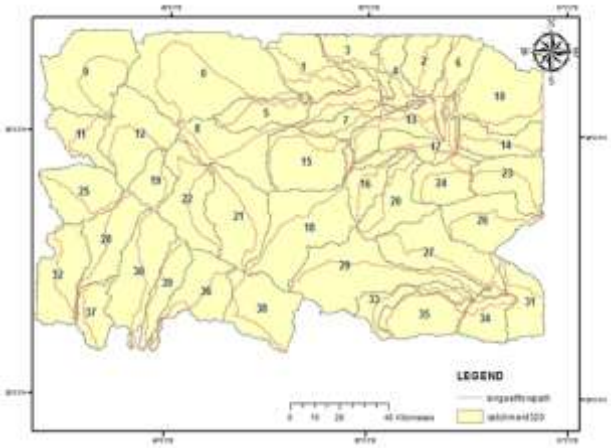

Figure 2. Drainage basins formed in this study area

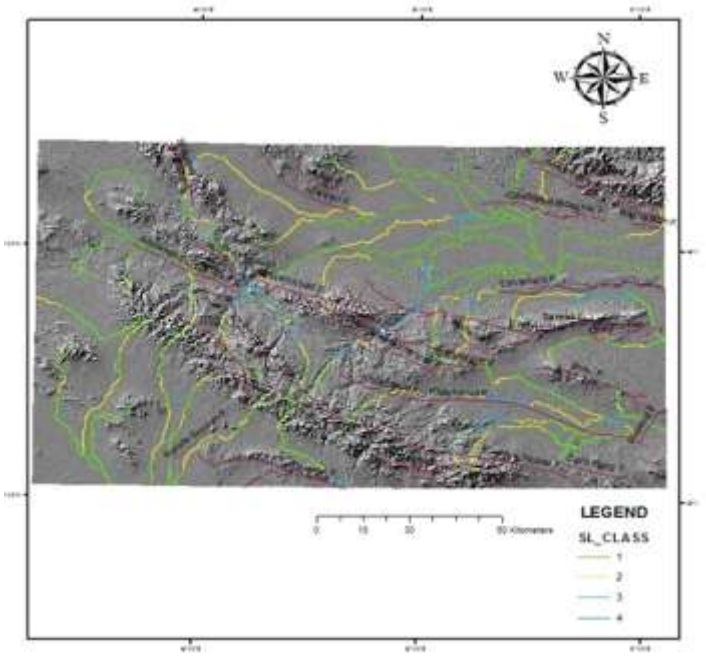

Figure 3. Classification of extracted waterways from the digital elevation model of the study area

3. Morphotectonic Indices

3.1. River Longitudinal Gradient Index (SL)

Longitudinal gradient index (SL) is one of the morphometric indices that represents the relationship between erosion and river flow. This index is also related to the power of the river (Hack, 1973; Hack, 1982). Because of SL's sensitivity to river bed slope changes, this index can be used as an effective and suitable tool for estimating river flow turbulence (Troiani and Della Seta, 2008). The SL index equation is computed by the formula [Hack, J. T. (1982) ,Hare, P. W., & Gardner, T. W. (1985) ,Keller, E. A. (1986) , Keller, E., & Pinter, N. (1996)]:

$SL= (\Delta H/\Delta Lr)\ Lsc$

Where, SL represents the longitudinal gradient of the river, $(\Delta H/\Delta Lr)$ represents the channel gradient of the river and Lsc represents the total length of the river channel from the starting point of the index to the highest point of the canal. In addition, SL index can also be used to estimate relative tectonic activity (Keller and Pinter, 2002). To calculate this index, a digital elevation model (DEM) with a precision of 30 meters along any flow path and for all the basins in the Arc GIS 10.1 software has been used.

Finally, the average values of this index for each sub-basin are also calculated. Here, in order to calculate the SL index for each of the existing floodplains in the 40 sub-basins, the scope is studied. The topographic layers of the digital elevation model with a precision of 30 meters to the layer of streams were added to the Arc GIS 10.1 environment and the values Lsc and $(\Delta H / \Delta Lr)$ were measured. As a result, SL values are smaller than 300 green, 500-300 yellow, 950-500 bright blue, 1550-950 blue, dark blue, 3000-1550 violet, and more than 3000 red (El Hamdouni et al, 2007). At the end, the channel layers with values of SL index were placed on the digital elevation model and the longitudinal gradient map of the river was studied in the studied area (Fig. 4). According to the

prepared map, the highest values of SL in the basins (0, 6, 12, 22 and 29) are measured, which is influenced by the effects of the Kooshk-eNosrat, Hasan Abad, Ipak and Soltanieh faults.

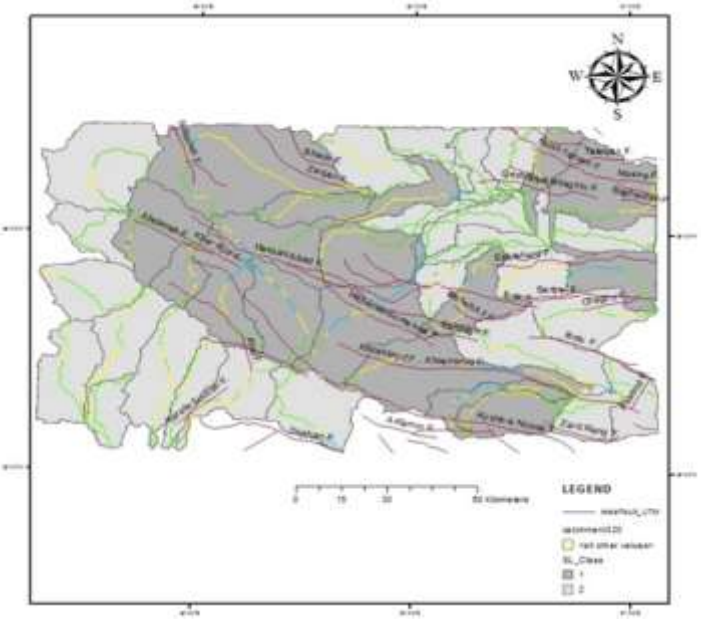

Figure 4. SL index map on a wide-ranging digital elevation model

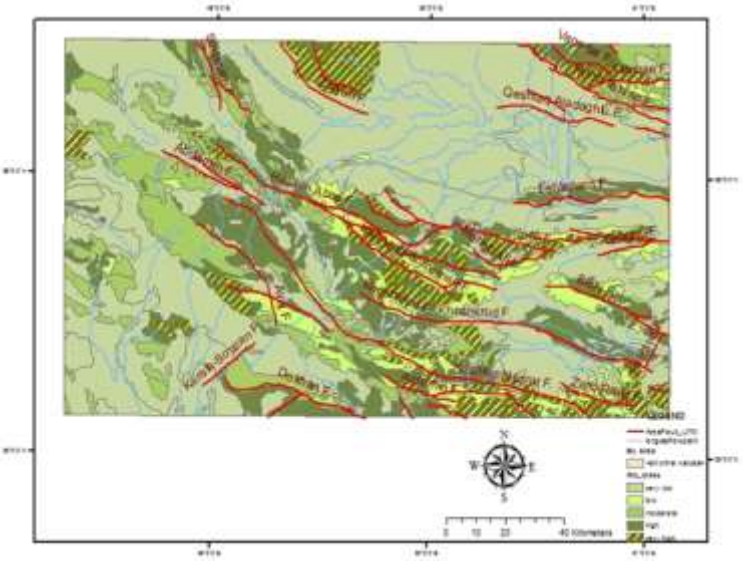

Figure 5. Distribution Map of SL Index Anomaly Values on Different Resistance Stones

In Fig. 5, the distribution map the of SL anomaly values on different resistance rocks is digitalized by recording anomalous values on a geology map of 1: 100,000 (Geological Survey of Iran). Considering the lithology of the valley cliffs of the river, the large amounts of the above-mentioned SL

anomalies can be interpreted as landmarks. Given the available data and geological map, the high values of the anomaly of the SL index are consistent with the faults of Kooshk-e-Nosrat and Hasanabad faults.

3.2. Asymmetry of Drainage Basin (AF)

Asymmetry factor of drainage basin (AF) is used to assess and evaluate the tilting of the basins. The geometric shape of the riverside network can be described quantitatively and quantitatively in several ways. The asymmetry factor can be computed using the following relationship:

AF =100 (Ar/At) (Hare and Gardner, 1985; Keller and Pinter, 2002)

Where (Ar) represents the area to the right of the basin relative to the main river (downstream) and (At) represents the total area of the drainage basin. If the result of calculating the drainage asymmetry index is close to 50, it indicates that the basin has a constant condition without a slight tilting or with a slight tilting. If the value of this indicator is larger or smaller than 50, then the basin is tilted, and it can be inferred that the basin is affected by the tectonic activity or is influenced by the linguistic characteristics and characteristics of the area. In general, for a drainage network in a basin where there is a continuous flow in a constant state, the value of this index should be 50. This index is related to bending perpendicular to the main drainage in the affected basin. If more bending is in the opposite direction, AF is less than 50. Most of the morphotectonic indices provide better results in regions and basins with similar lithological conditions. when calculating the AF index and analyzing the results, the effects of lithological controllers and climatic conditions are not taken into account.

In this study, the asymmetry factor of drainage basin and the area of the right area of the basin (Ar) and the total area of drainage basin (At) in Arc GIS 10.1 software were calculated and AF in 40 drainage basins in the study area were studied and measured. The value of this indicator varies from 15 (in basin 6) to 85 (in basin 10). After calculating this index for all basins, the results of these values were classified in three classes 1, 2 and 3. class 1 with a range of Af≥65 or Af<35 represents the high levels of basin tilt, or 57≤Af<65 represents the mean values of deviation and class 3 with a range of 43≤Af<57 represents the low values of basin tilting (Dehbozorgi et al, 2010). Consequently, the basin asymmetry map was prepared and produced by using Arc GIS 10.1 software (Fig. 6). The highest values of this indicator were measured in basins (3, 5, 6, 9, 10, 14, 15, 18, 19, 20, 22, 27, 28, 31, 34, 35, 37, 38 and 39).

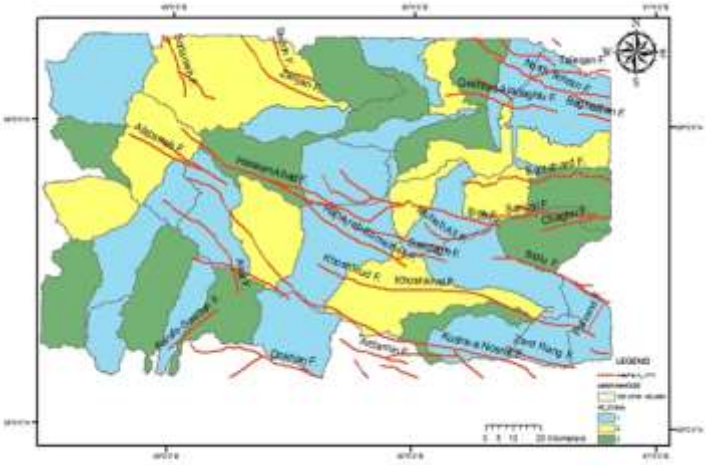

Figure 6. Drainage basin asymmetry map in the study area

3.3. Hypsometric and Integral Hypsometric Curve (Hi)

Hypsometric integral shows the distribution of altitude levels in a region and basin (Strahler, 1952). The Hi index describes the area of the lower surface of the hypsometric curve, thus indicating the capacity of an eroding basin. One of the simple methods for describing the shape of the hypsometric curve of a basin is to calculate its hypsometric integral. Hypsometric integral of the basin is obtained by using the area of the lower surface of the hypsometric curve. The equation used to calculate the hypsometric integral is as follows (Bull, 2007; Keller and Pinter, 2002; Mayer, 1990):

Hi = (Average elevation – min elevation / max elevation – min elevation).

In this index, the minimum, maximum and mean height were calculated from a digital elevation model (DEM) with accuracy of 30 m using Arc GIS version 10.1. After calculating the Hi index for all drainage basins, this index is classified in three classes (El Hamdouni et al, 2007). Class 1 contains convex curves or kluge with an integral hypsometry greater than 0.5 ($Hi \geq 0.5$). This category of hypsometric curves with high values indicates the topography of the basin above its mean value. Class 2 contains convex-concave curves ($0.4 \leq Hi < 0.5$). This is the intermediate between class 1 and class 2. And Class 3 includes concave curves with hypsometric integral values less than 0.4 ($Hi < 0.4$), This category represents the cut off the drainage network at levels with a mild topography than the first one. To form the hypsometric curve of a drainage basin, we plot the total height of the area in relation versus the total area of the basin. Due to the fact that in the hypsometric curve, the area and height of the basin are divided into the total area and height of the basin, the numbers are dimensionless, Therefore, the hypsometric curves are independent of area and height. Therefore, these types of curves can be compared with each other in terms of size, height, and area. Hence, due to this feature of hypsometric curves, topographic maps can be used in different scales. The relationship between the hypsometric integral and the cutoff value of drainage networks is used as an indicator for determining the erosion cycle of landscapes in the region. This cycle occurs during several stages, which are: youth stage, maturity and aging.

The young stage in this cycle is characterized by deep cuts and uneven prominences. In the stage of maturity, we see a balance in geomorphologic processes. An aging stage is described with close-to-surface scenarios and very closely related prominences. Therefore, hypsometric curves, which are very important in posterior and vertical evaluation, are in particular importance as an efficient method for identifying active and passive tectonic areas. Hypsometry integrals have been measured in 40 basins in the study areas. The minimum value of the measured hypsometric integral belongs to basin number 23 with the value (0.11), the shape of the curve for which it is concave, and the maximum value of this integral is obtained in basin number 7 with the value (0.55) and the convex curve. In Figure 7 according to the Hi level, the sub-basins are divided into three categories 1, 2, and 3, which respectively represent the high, middle and bottom tectonic activity.

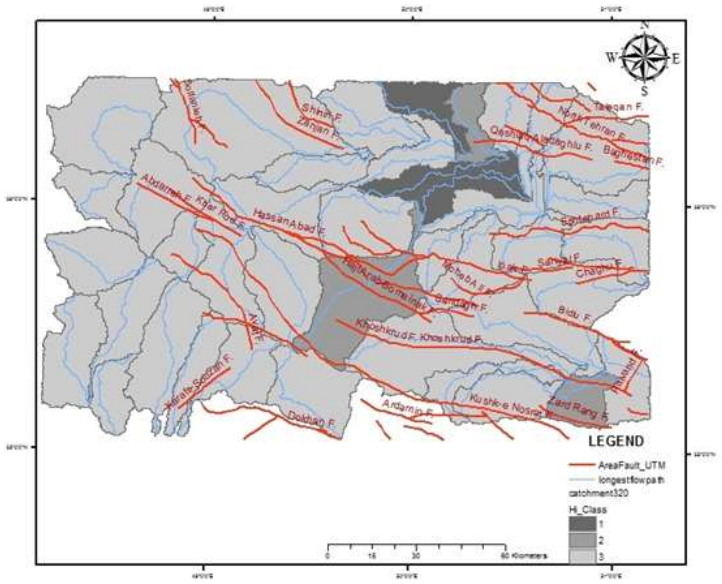

Figure 7. Sub-basin classification map based on the Hi index in the study area.

As is clear from this figure, the basins with activities 1 and 2 are located within the fault zones of Aladaghloo, Kooshk-e-Nosrat, Hasan Abad, Khoshkrud, Hajj Arab, Koorcheshmeh, Sari Dareh-Hajj Arabs. In general, a large part of the area shows a low activity category, indicating that the area studied has a low sensitivity to the hypsometric index. In other words, there is no significant difference in height between sub-basins.

3.4. Drainage Basin Form (Bs)

During the tectonic processes, the shape of the basin may change. The basin shape indicates the difference between basins with significant elongation, and the basins which their shapes are close to the circle. The horizontal image of a basin can be described by the shape of the basin or the elongation ratio (Ramírez-Herrera, 1998). In regions that are active, the basins are more elongated and have high levels of this index, in contrast, in the areas with lower tectonic activity, the elongation of the basins decreases and their shape becomes closer to the circle and the value of Bs decreases (Bull, 2007). The drainage basin shape index (Bsc) is determined by using the following equation (Ramírez-Herrera, 1998; Cannon, 1976):

$$Bs = Bl/Bw$$

Where Bl represents the length of a basin in the main drainage path that is calculated from the point of drainage from the basin to the highest point in the basin, Bw is the width of the basin, which is measured at the widest part of the basin, that is parallel to the length of the basin (Bl). The Bs index was measured for all basins and the results were ranked in three classes including: class 1 of tectonic activity ($Bs \geq 4$), class 2 of tectonic activity ($3 \leq Bis < 4$) and class 3 of tectonic activity ($Bs \leq 3$) (El Hamdouni et al, 2007). The amount of tectonic activity in the first class is the highest and in the third class is the lowest. The results of calculating the Fbs index in 40 basins have been studied. The range of results for this indicator varies from 1.69 (range 19) to 11.35 (in basin 33). Approximately 60% of the studied basins are close to the circle and belong to class 3 tectonic activity. In the map derived from the measurement of the shape of the basin (Fig. 8), there are several focusing centers of the underlying

basins.

Because the trapped sub-basins, which have the class 1, represent tectonic activity in that basin, the focus of these sub-bases around a fault can be attributed to its quaternary activity of that fault. The highest concentration is under the drainage basins in the vicinity of Kooshk-e- Nosrat, Khoshkrud, Hasanabad, karafs-Suzan, Bidoo, Koorcheshmeh, Haj-Arab-Seminak, Moheb Ali, Eshtehard and Gheshlag Aladaghlu. In general, according to the results of measurements of the drainage index of the basin, the activity of Kushk-e-Nosart and Hassanabad faults has been much higher in the production of highly active basins and indicates the greater activity of these faults than other faults in the studied area.

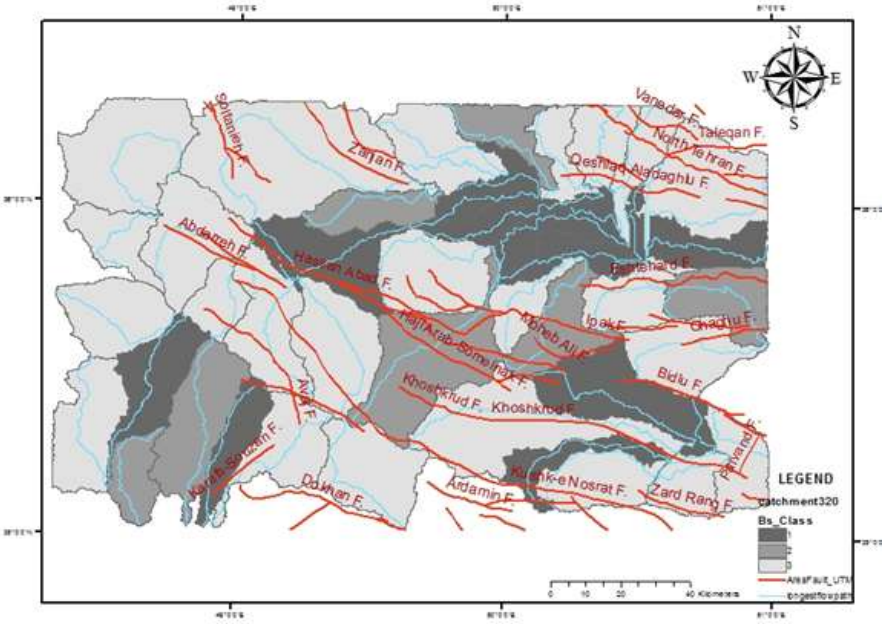

Figure 8. Sub-basin classification map based on the Bs index in the study area.

3.5. The Ratio of the Width to Height of the Valley (Vf)

This index is one of the morphometric indices that affects tectonic uplift and is sensitive to this factor. This indicator is defined as the ratio of the bottom of the valley to the valley height as follows:

$Vf = Vfw/ [(Ald-Asc) + (Ard-Asc) /2)]$

Where (Vf) represents the ratio of width to height of the valley, (Vfw) represents width of the valley, (Asc), (Ald), (Ard) represents the height of the dividing line in the right, left and the bottom of the valley, respectively (Bull, 2007). Normally, high values of the Vf index are consistent with tectonic uplift rates (Keller & Pinter, 2002). After calculating the Vf index in the range of studies, this index is graded in three classes, the three classes are: class 1 ($Vf \leq 0.5$), this category of the Vf index represents V-shaped valleys, class 2 ($0.5 \leq Vf < 1.0$), this category of Vf represents an intermediate state of the valley between classes 1 and 3, and finally, class 3 ($Vf \geq 1$) represents U-shaped valleys (El-Hamdouni et al, 2007). The Vf index range in this study varies from 2.65 (in basin 36) to 15.27 (in basin 16). The results of measuring this index indicate that most of the valleys measured in the study area are U shaped. Figure 9 represents sub-basins map based on the Vf index in the study area. As shown, according to the classification of this index, the area has U-shaped valleys.

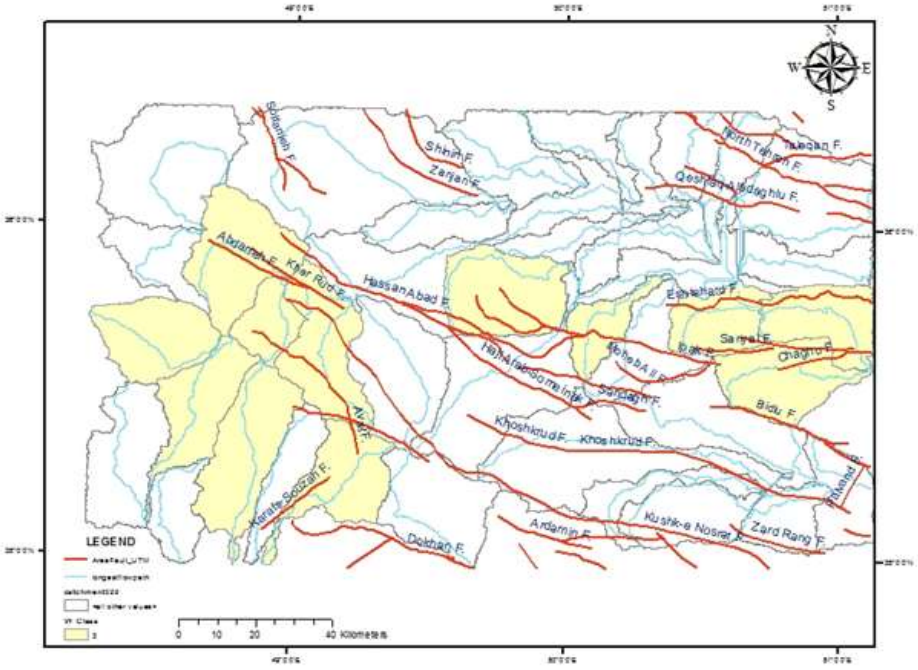

Figure 9. Sub-basin classification map based on the Vf index in the studied area.

3.6. The Twist to Mountain Front (Smf)

This index describes the equilibrium between river erosion processes that tend to cut into the border between the mountains and the plains and describes active tectonic forces that tend to produce a direct mountain front along with faulting (Bull and McFadden, L.D., 1977; Keller, 1986). This index is calculated using the following equation (Bull, 2007):

(J) (Smf) = Lj/Ls

Where Smf is the index of mountain front and the plains sinusitis, Lj is the length of the mountain front along the foothills and Ls is the length of the straight line of the mountain front.

This index is usually less than 3 and close to 1, where a steep sloping mountain suddenly rising along the mountain front (Bull, 2007). Uplifted mountain fronts resulted from tectonic activities are directly and smoothly, and this index value is low for them. But if the height of the mountain front elevation decreases or the uplifing is stopped, mountain front will affect by erosion processes, and become sinusoidal shape and its twist rises, so, the value of the index J will also increase. this index can be calculated by use of data from topographic maps or satellite images. Large-scale maps and high-resolution satellite images can be used to accurately measure this index. This index has been surveyed for 31 mountain fronts and after calculating the indices, they are classified in three tectonic classes. this classification, including class 1 with J <1.10, class 2 with 1.50> J ≥ 1.10 and class 3 with J ≥ 1.50 represents the tectonic activity of the region (El-Hamdouni et al, 2007). The lowest value of the index of mountain front in this study is about 1 that is related to basins 0, 8, 15, 16, 18, 21, 24, 25, 26, 28, 30, 36 (Fig. 10).

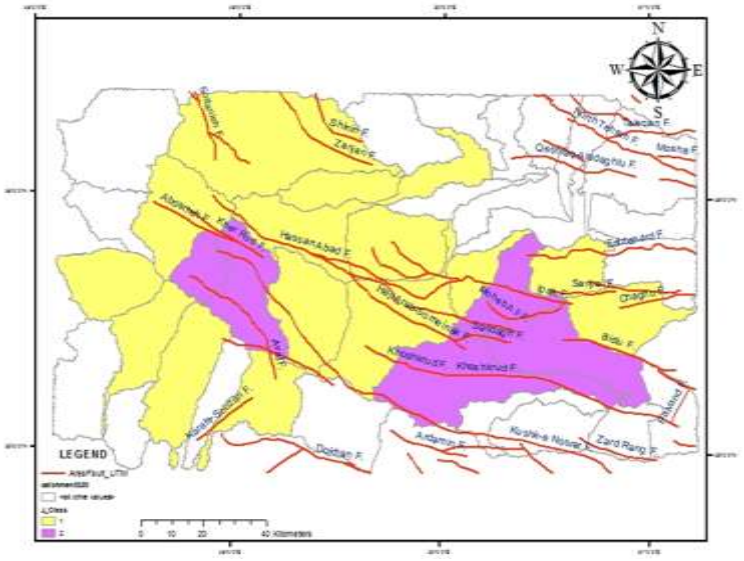

Figure 10. Sub-basin classification map based on the index of the J-mountain the border between the mountains and the plains index.

3.7. Index of Relative Active Tectonic (IAT)

In most tectonic studies, the index relative active tectonic is calculated by two main indices and studies usually focus on the mountain front or river basins (Bull and McFadden, 1977; Azor et al., 2002; Rockwell et al., 1985). In the present study, a number of geomorphic indicators have been analyzed throughout the region to estimate tectonic activity, including longitudinal gradient of the river, asymmetry of drainage basin, hypsometric integral, ratio of drainage basin shape, the ration of the width to the height of the valley and the index of twist of mountain front. The index of relative active tectonic can be calculated by S/n relationship using the mean values of each category of morphotectonic indices in all basins. To characterize the intensity and degree of tectonic activity, this index is distributed in 4 tectonic classes: class 1 of relative active tectonic ($1.0 \leq Iat < 1.5$) represents a very high tectonic activity. Class 2 ($1.5 \leq Iat < 2.0$), represents a relatively high tectonic activity. Class 3 ($2.0 \leq Iat < 2.5$) represents an intermediate tectonic activity and finally, class 4 ($2.5 \leq Iat$) reflects a relatively low tectonic activity. Finally, after classifying the relative active tectonic values, the distribution map of the tectonic activity of the area was arranged in Arc GIS 10.1 software environment and the study area was divided into four sections: very active, active, moderate activity and low activity (Fig. 11). Analyzing the results of the classification of the relative active geochemical index that 30% of this study are very high and high tectonic activity in the area and located in the class 1 and 2 of the Iat index, and about 65% is in class 3, indicating moderate tectonic activity in the region. About 5% of the area study is in the category of 4 Iat index, which indicates low levels of tectonic activity in the studied area (Table1).

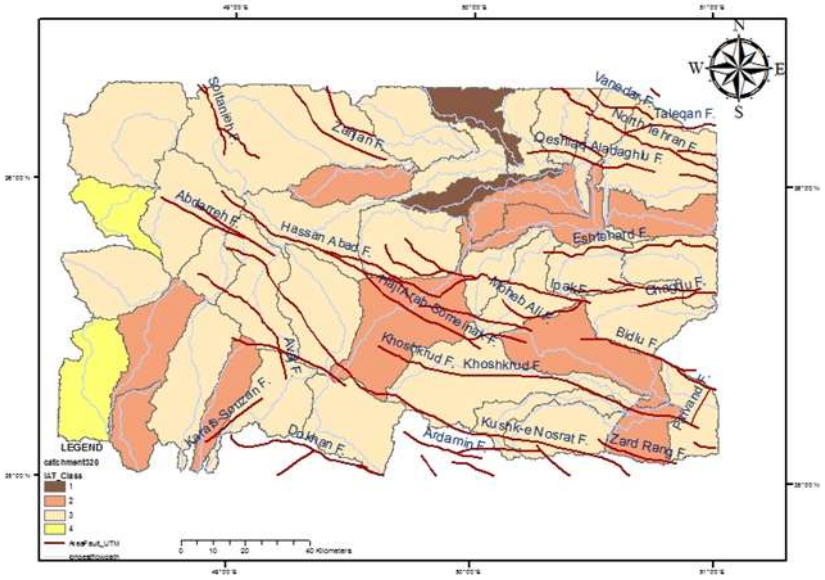

Figure 11. Relative tectonic activity level (Iat) distribution map in the study area.

Table 1. Tectonic activity value and category of morphotectonic indices in 40 drainage basins.

FID	Area	Af_Class	Bs_Class	Hi_Class	J_Class	SL_Class	Vf_Class	IAT	IAT_Class
0	1641/212524	2	3	3	1	2	-	2/2	3
1	545/702289	3	3	3	-	1	-	2/5	3
2	350/639366	3	3	3	-	1	-	2/5	3
3	317/617636	1	2	1	-	1	-	1/25	1
4	264/434992	2	3	2	-	1	-	2	3
5	358/599114	1	2	3	1	2	-	1/8	2
6	309/773686	1	3	3	-	2	-	2/25	3
7	241/304846	1	1	1	-	1	-	1	1
8	956/524916	3	1	3	1	2	-	2	3
9	944/198369	1	3	3	-	1	-	2	3
10	894/565547	1	3	3	-	2	-	2/25	3
11	343/786493	3	3	3	-	1	-	2/5	4
12	695/602212	2	3	3	1	2	3	2/33	3
13	364/197371	3	1	1	-	1	-	1/5	2
14	354/977416	2	1	3	-	1	-	1/75	2
15	654/506532	1	3	3	1	2	3	2/17	3

16	273/150224	2	3	3	1	1	3	2/17	3
17	366/708201	2	1	3	-	1	-	1/75	2
18	1008/171034	1	2	2	1	2	-	1/75	2
19	259/906074	1	3	3	2	2	3	2/33	3
20	474/495015	1	2	3	2	2	-	2	3
21	703/807133	2	3	3	1	2	-	2/2	3
22	625/493026	1	3	3	2	2	3	2/33	3
23	474/625188	3	2	3	-	2	3	2/17	3
24	382/191654	2	3	3	1	1	3	2/17	3
25	542/402432	2	3	3	1	1	3	2/17	3
26	566/700945	3	3	3	1	1	3	2/33	3
27	761/140952	1	1	3	2	1	-	1/6	2
28	516/578575	1	1	3	1	1	3	1/67	2
29	1058/94507	2	3	3	2	2	-	2/4	3
30	711/359588	3	2	3	1	1	3	2/17	3
31	372/03493	1	3	3	-	1	-	2	3
32	599/493474	3	3	3	-	1	-	2/5	4
33	289/064927	3	1	3	-	2	-	2/25	3
34	303/544527	1	3	2	-	1	-	1/75	2
35	458/759999	1	3	3	-	2	-	2/25	3
36	524/985544	3	3	3	1	1	3	2/33	3
37	287/044444	1	2	3	-	1	-	1/75	2
38	622/446328	1	3	3	-	1	-	2	3
39	324/15426	1	1	3	-	1	-	1/5	2

4. Seismotectonic of the Study Area

The seismic history in the study area shows that towns like Buin Zahra have been repeatedly destroyed. Numerous earthquakes in the study area are a sign of its seismicity. According to the earthquake risk zoning map in Iran and according to the seismic characteristics, the area falls in the high risk to moderate risk areas. (Aghanabati, 2004) The distribution of historical and instrumental earthquakes in the area, shown in Figure 12, can be distinguished by magnitude, and as can be seen from the map, the distribution of earthquakes is in accordance with the trend of the main faults in the region. Earthquakes with a magnitude of 3.6 to 4 are more extensive. The seismic parameters of the studied area are summarized in Table 2.

Table 2. Seismic parameters of the study area

	Mmax	Mmin	b	a	λ	β
Zone	7.40	2.90	0.68	2.99	2.34	1.56

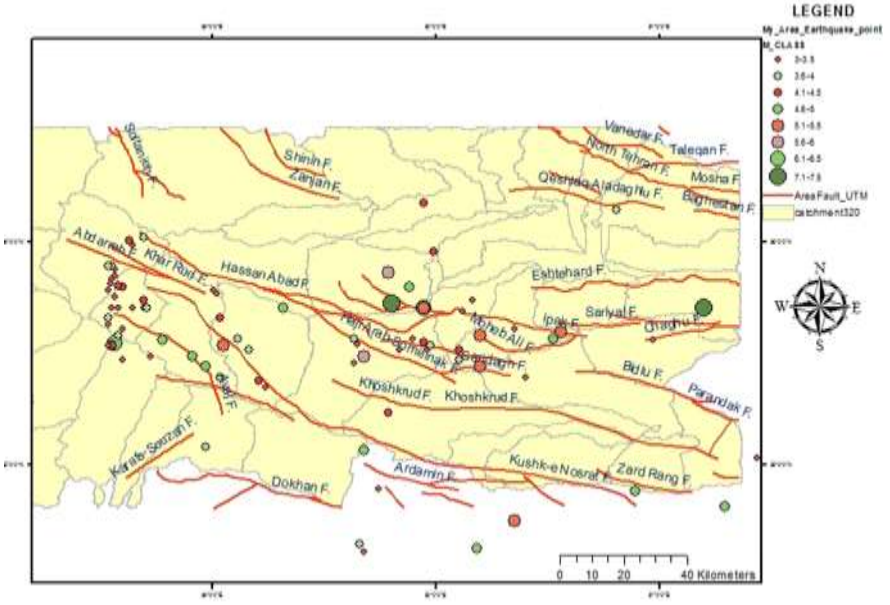

Figure 12. Distribution of historical and instrumental earthquakes in the studied area

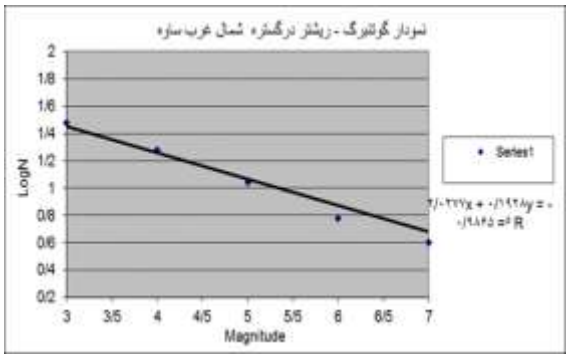

Figure 13. Gutenberg-Richter seismic diagram in the study area

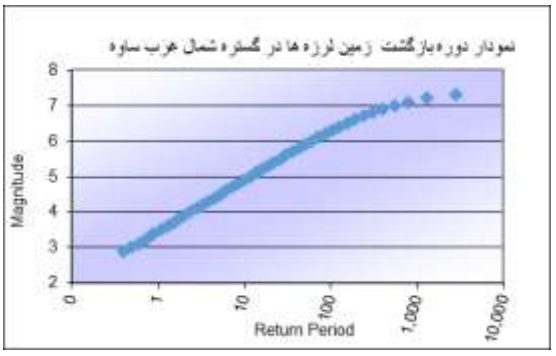

Figure 14. Graph of the return period of earthquakes in the study area

5. Earthquake Return Period

After calculating the seismicity parameters, using the Kijko-Sellevoll-Graham method, the return period of earthquakes is calculated for the design range. By calculating the return period of

earthquakes, it is possible to determine the annual rate of an earthquake event of a certain magnitude. Figure 14 shows the seismic rhythm of the area which states that the largest possible earthquake in the area has a return period of 2800 years.

6. Seismic Potential of Active Faults in the Study Area

There are two ways to estimate the maximum magnitude created by each fault:

A) The use of seismicity history and earthquakes attributed to that fault

B) Using the experimental relationships between the magnitude and length of fault rupture by various researchers in this study, the Mohajer-Ashjaei and Nowroozi (1985) and Zare (1999) and Wells and Coppersmith (1994) and Ambraseys and Jackson (1998) relationships for calculation of the maximum seismicity of the active faults in the study area is used.

Table 3. Seismic capacity of active faults in the region

ZONE	F. Name	Lf	Z.LR=%37Lf	Zare	N.LR=%50Lf	Norowzi	Copper	Am	Avg.
0	Khoshkrud F.	80	29/6	6/7	40	7/0	6/9	7/2	7/0
1	Khoshkrud F.	25	9/25	5/7	12/5	6/5	6/4	6/7	6/3
2	Parandak F.	34	12/58	6/0	17	6/6	6/5	6/9	6/5
3	Bidlu F.	38	14/06	6/1	19	6/7	6/6	6/9	6/6
4	Chaghu F.	41	15/17	6/1	20/5	6/7	6/6	6/9	6/6
5	Dokhan F.	47	17/39	6/3	23/5	6/8	6/7	7/0	6/7
6	Qeshlaq-Aladaghlu F.	42	15/54	6/2	21	6/7	6/6	7/0	6/6
7	Nobaran F.	40	14/8	6/1	20	6/7	6/6	6/9	6/6
8	Soltanieh F.	132	48/84	7/2	66	7/2	7/2	7/5	7/3
9	Zanjan F.	143	52/91	7/3	71/5	7/3	7/2	7/5	7/3
10	Indes F.	110	40/7	7/0	55	7/1	7/1	7/4	7/2
11	Kooshk-e Nosrat F.	221	81/77	7/7	110/5	7/4	7/5	7/7	7/6
12	Mosha F.	215	79/55	7/6	107/5	7/4	7/4	7/7	7/6
13	Vanedar F.	28	10/36	5/8	14	6/5	6/4	6/8	6/4
14	Sariyal F.	21	7/77	5/5	10/5	6/4	6/3	6/6	6/2
15	Khan Kish F.	22	8/14	5/6	11	6/4	6/3	6/7	6/2
16	Khar Rud F.	30	11/1	5/9	15	6/6	6/4	6/8	6/4
17	Chopoghlu F.	18	6/66	5/4	9	6/4	6/2	6/6	6/1
18	Darejin F.	17	6/29	5/3	8/5	6/3	6/2	6/5	6/1
19	Baghestan F.	34	12/58	6/0	17	6/6	6/5	6/9	6/5
20	Moheb Ali F.	28	10/36	5/8	14	6/5	6/4	6/8	6/4
21	Qermez Aghash F.	14	5/18	5/2	7	6/2	6/1	6/5	6/0
22	Bagher Abad F.	15	5/55	5/2	7/5	6/3	6/1	6/5	6/0

23	Zard Rang F.	26	9/62	5/7	13	6/5	6/4	6/7	6/3
24	Omar Abad-Khianak F.	40	14/8	6/1	20	6/7	6/6	6/9	6/6
25	North Tehran F.	12	4/44	5/0	6	6/2	6/0	6/4	5/9
26	North Tehran F.	17	6/29	5/3	8/5	6/3	6/2	6/5	6/1
27	No name	17	6/29	5/3	8/5	6/3	6/2	6/5	6/1
28	Eshtehard F.	34	12/58	6/0	17	6/6	6/5	6/9	6/5
29	Ipak F.	38	14/06	6/1	19	6/7	6/6	6/9	6/6
30	Hassan Abad F.	43	15/91	6/2	21/5	6/7	6/6	7/0	6/6
31	Avaj F.	35	12/95	6/0	17/5	6/6	6/5	6/9	6/5
32	Ahmad Abad-Karvansara F.	39	14/43	6/1	19/5	6/7	6/6	6/9	6/6
33	Ardamin F.	26	9/62	5/7	13	6/5	6/4	6/7	6/3
34	Abdarreh F.	30	11/1	5/9	15	6/6	6/4	6/8	6/4
35	Neshveh F.	27	9/99	5/8	13/5	6/5	6/4	6/8	6/4
36	Kour Cheshmeh F.	6	2/22	4/4	3	5/9	5/6	6/1	5/5
37	Saridarreh-Haji Abad F.	15	5/55	5/2	7/5	6/3	6/1	6/5	6/0
38	Haji Arab-Someinak F.	42	15/54	6/2	21	6/7	6/6	7/0	6/6
39	Gomrokan F.	7	2/59	4/5	3/5	5/9	5/7	6/1	5/6
40	Paivand F.	13	4/81	5/1	6/5	6/2	6/0	6/4	5/9
41	Avaj F.	11	4/07	4/9	5/5	6/1	5/9	6/4	5/8
42	Shinin F.	10	3/7	4/9	5	6/1	5/9	6/3	5/8
43	North Tehran F.	15	5/55	5/2	7/5	6/3	6/1	6/5	6/0
44	Alborz F.	93	34/41	6/9	46/5	7/1	7/0	7/3	7/1
45	Karafs-Souzan F.	23	8/51	5/6	11/5	6/5	6/3	6/7	6/3
46	North Qazvin F.	101	37/37	7/0	50/5	7/1	7/1	7/4	7/1
47	Taleqan F.	19	7/03	5/4	9/5	6/4	6/2	6/6	6/2

7. Seismic Hazard Analysis with Deterministic Approach

Seismic Hazard analysis consists of four main steps, which are:

1- Identification of seismic sources

2- Determining control earthquake for each fault

3- Selecting reduction relations for ground movement parameters

4- Calculating the ground movement design parameters

The values of maximum Magnitude, minimum distance, and some other parameters is provided in Table 4.

In this study, the reduction relations proposed by Zare (1995) and Zare (1999) have been used. The results show that Kooshk-e- Nosrat fault has the highest acceleration (horizontal acceleration: 7.19 m/s^2 and vertical acceleration: 3.5 m/s^2). The highest acceleration calculated in the region is related to

Kooshkk-e-Nosrat, Alborz, Khoshkrud, Zardrang and Indes faults.

Table 4. Profile of seismic sources in the study area

No.	Fault Name	Fault Length (Km)	Fault type	Mw	Total HPGA	Total VPGA
1	Avaj	46	Historical Earthquakes & Seismic	6/7	0/8834	0/3133
2	Aipak	38	Historical Earthquakes & Seismic	7/2	2/4587	0/9665
3	Indes	110	Seismic	7/2	3/3226	1/394
4	Paivand	13	Active	5/9	1/6813	0/7217
5	Hassan Abad	43	Seismic	6/6	1/279	0/476
6	Haji Arab-Someinak	42	Abundant Micro Earthquake	6/6	1/7806	0/7043
7	Sarydare Hajiabad	15	Abundant Micro Earthquake	6	1/2709	0/5024
8	Soltaniyeh	132	Seismic	7/3	0/7309	0/2749
9	North Tehran	44	Seismic	6/6	0/7994	0/2819
10	North Qazvin	101	Seismic	7/1	0/8828	0/3179
11	Taleqhan	19	Seismic	6/2	0/5705	0/1985
12	Kushk-e-Nusrat	221	Abundant Micro Earthquake	7/6	7/1974	3/5043

8. Seismic Networking of the Study Area and Isoacceleration Map

In the present study, after selecting points with regular distances and determining the network of points in the study area, the length of faults, the distances of each fault to the points of the seismic network, the maximum seismicity of each fault and The maximum seismicity was calculated in and finally the horizontal and vertical acceleration resulted of each fault in the points related to the seismic network was calculated so that we will have 47 Horizontal Accelerations and 47 Vertical Accelerations for each point of the seismic network (for each fault at any point, one Horizontal Acceleration and one Vertical Acceleration). Finally, the acceleration curves of the region were drawn using Arc GIS software.

Figures 16, 17 and 18 show the Horizontal, vertical and General Acceleration in the region along with the position of faults and vibrations occurring in the study area. As can be seen, increase in acceleration in the area follows the general direction of faults in the area and major parts of the north and northwest of Saveh are located in the area of maximum calculated acceleration, which is important in terms of seismic hazard considerations, and deserves a much attention of authorities in terms of strengthening and preventing the establishment of strategic structures.

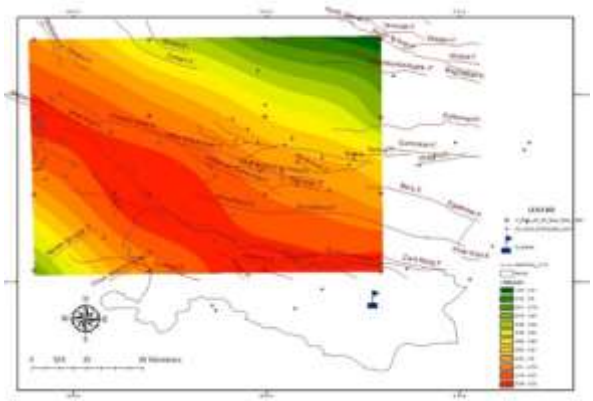

Figure 15. Iso-acceleration contours corresponding to the Horizontal Acceleration in the studied area.

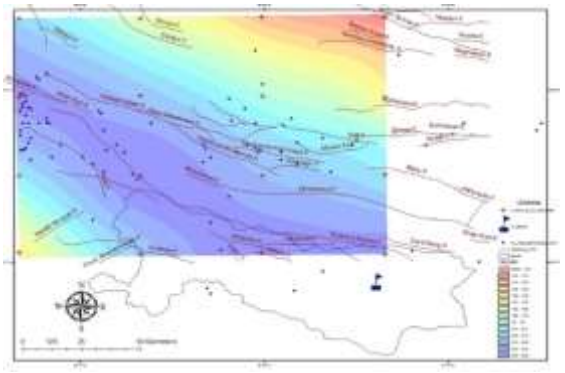

Figure 16. Iso-acceleration contours corresponding to the Vertical Acceleration in the studied area.

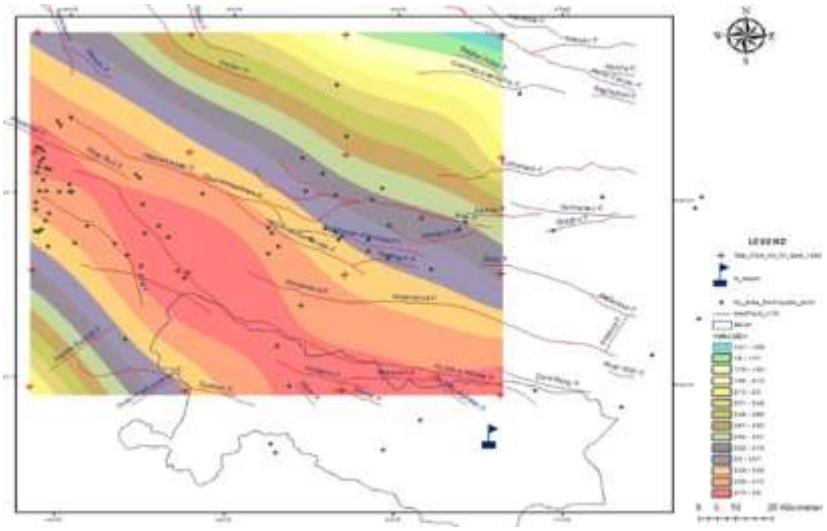

Figure 17. Iso-acceleration curve related to the overall acceleration in the study area

9. Discussion and Conclusion

Based on SL index calculations, basins 0, 5, 6, 8, 10, 12, 14, 15, 18, 19, 20, 21, 22, 23, 29, 33 and 35 have activity level 1 and show the highest SL rate. These basins are located on the Ipak, Hasanabad, Kooshk-e- Nosrat and Soltanieh faults. The activity level is 2 and have lower SL rate in the parts of the study area.

The highest SL values were measured in basins 0, 6, 12, 22, and 29, which are influenced by the effects of Kooshk-e-Nosrat, Hassanabad, Ipak and Soltanieh faults. Because the rivers of the area are completely in line with the fault zones, in areas with no major faults, the rivers with high SL cannot be seen, and so the results can be more valid.

Based on the results obtained from Af calculation, basins with class 1 of tectonic activity are developed in most areas, whether in plains or in highlands. Most of the 1st and 2rd class basins with maximum tilting are concentrated around the main faults, such as Kooshk-e-Nosrat, Hassanabad, Avaj and Ipak, which in turn, represents recent quaternary activities.

An examination of the hypsometric index in the region, shows that a large part of the region has a low activity category and this suggests that this study had a low sensitivity to the hypsometric index. In other words, there is no significant difference in elevation between basins.

According to the calculations related to the index of basin elongation (Bs), the activity of Kooshk-e-Nosrat and Hasanabad faults has been much more effective in forming highly active and elongated basins, which indicates the greater activity of these faults compared to the other faults is study area.

The results of Bs index show that approximately 60% of the studied basins are close to the circle-shape and belong to class 3 tectonic activity.

The classification of sub-basins based on the Vf index in this studied, shows that the area has U-shaped valleys.

Examining mountain front by hill shade pictures and its elevation meters, show that the sub-basins adjacent to or along the main faults have the highest rate of J activity, also, the main focus of the active sub-basins is in terms of sinusoidal rate of the mountain front along the Kooshk-e-Nosrat, Hassanabad, Avaj, Haj Arab Seminek, Soltanieh and Zanjan faults.

Analyzing the results of the classification of the activated particulate land index shows that 30% of the study area show high to very high tectonic activity, which fall in class 1 and 2 of the Iat index, whereas about 65% fall in class 3, which represents moderate tectonic activity. About 5% of the study falls in class 4 of IAT index, which reflects low levels of tectonic activity in the that part of the study area.

Given to the analysis of the index of relative active tectonic in the studied area, Aladaghlu, Eshtehard, Kooshk-e-Nosrat, Khoshkrud, Hassanabad, Ipak, Haj Arab Seminak, Moheb Ali, Bidoo, Zardrang, Ahmadabad Caravansara and Karafs-Suzan faults, has very high to high relative activity and Soltanieh-Darjezin, Zanjan, Abdareh, Avaj and Baqerabad faults show moderate relative tectonic activity. In the meantime, a fault with a relatively small tectonic activity is not observed, and in general, the entire zone can be considered tectonically active.

Among the indices calculated for the studied area, the AF, SL, and J indices had the highest activity rates, indicating the sensitivity of these indices to the type of dominant movement in this zone. Nearly all of the faults in this area are dominated strike-slip with reveres movements, like the Kooshk-e-Nosrat's fault, which is a thrust with a dominant strike-slip component.

Major and large faults include Kooshk-e-Nosrat, Hassan Abad, Ipak, Khoshkrud, Haj Arab Senimak, and the basins corresponding to these faults, which embrace a large number of basins, all have a of high or very high level of relative tectonic activity which indicates the high tectonic activity of these faults in the Quaternary. Kooshk-e-Nosrat, Hassanabad and Haj Arab faults are the most important and most severe faults in the region, because almost all of the basins have high IAT.

In Basin 18, where the bending of the Kooshk-e-Nosrat fault points to the southeast, the highest quaternary activity rate has been shown in all measured indices.

In the study area, the distribution of earthquakes is consistent with the trend of the main faults in the area. Earthquakes with a magnitude of 3.6 to 4 are more extensive.

The plotted seismic return period diagram shows the seismic rhythm of the region and states that the largest possible earthquake in the region has a return period of 2800 years.

Kooshk-e-Nosrat fault with a length of 221 km has the highest seismicity in the region and creates the maximum possible earthquake for the region.

Studies show that Kooshk-e-Nosrat fault has the highest amount of acceleration (horizontal acceleration: 7.19 m/s2 and vertical acceleration: 3.5 m/s2) in the area. Alborz, Khoshkrud, Zardrang and Indes faults and in the next having the highest acceleration in the area, respectively.

According to the acceleration maps of the study area and its integration with existing faults and earthquakes occurred in the study area, can be observed that the increase in acceleration in the area

follows the general direction of its faults.

Most of the north and northwest of Saveh City is located in area with calculated maximum acceleration.

10. Advice

Determining the amount of tectonic activity and identifying active faults in the studied area; Due to the fact that this area is one of the important industrial areas and has many important and densely populated cities Like Alborz, Qazvin, Markazi, and Hamadan are on the same border.

Avoid planning to build new structures or develop residential areas or industrial in the areas with relatively high tectonic activity or the central areas of earthquakes in the study area

Preparation of maps of population density and density of important industrial centers, and matching the results obtained from the level of tectonic activity and the risk of seismicity with these maps in order to predict the risks for this area and the level of damage caused due to the continuation of tectonic activities.

Crisis management in the study area and prevention of possible risks by preparing a map of the acceleration zones for the region and specifying the high-risk areas.

References

Aghanabati, A. (2004). *Geology of Iran*. Geological Survey of Iran.

Alavi, M. (1991). Sedimentary and Structural characteristics of the Paleo-Tethys remnants in northeastern Iran. *Geol. Soc. of Amer. Bull., 103*, 983.

Alavi, M. (1994). Tectonics of the Zagros orogenic belt of Iran: new data and interpretations. *Tectonophysics, 229*, 211-238.

Alavi, M. (1996). Tectonostratigraphic synthesis and structural style of the Alborz mountain system in northern Iran. *J. Geodyn., 21*, 1- 33.

Altin, T. B., & Altin, B. N. (2011). Development and morphometry of drainage network in volcanic terrain, Central Anatolia, Turkey. *Geomorphology, 125*, 485–503.

Azor, A., Keller, E. A., & Yeats, R. S. (2002). Geomorphic indicators of active fold growth: South Mountain–Oak Ridge Ventura basin, Southern California. *Geological Society of America Bulletin, 114*, 745–753.

Babaahmadi, A., Safaei, H., Yassaghi, A., Vafa, H., Naeimi, A., & Madanipour, S. (2010). A study of Quaternary structures in the Qom region, west central Iran. *Journal of Geodynamics, 50*(5), 355-367.

Bull, W. B., & McFadden, L. D. (1977). Tectonic geomorphology north and south of the Garlock fault, California, In: *Doehring, D.O. (Ed.), Geomorphology in Arid Regions, Proceedings of the Eighth Annual Geomorphology Symposium, State University of New York, Binghamton*, 115–138.

Bull, W. B. (2007). *Tectonic geomorphology of mountains: a new approach to paleo-seismology*. Blackwell, Malden.

Cannon, P. J. (1976). Generation of explicit parameters for a quantitative geomorphic study of Mill Creek drainage basin. *Oklahoma Geology Notes, 36*(1), 3–16.

Dehbozorgi, M., Pourkermani, M., Arian, M., Matkan, A. A., Motamedi, H., & Hosseiniasl, A. (2010). Quantitative analysis of relative tectonic activity in the Sarvestan area, central Zagros, Iran. *Geomorphology, 121*(3), 329-341.

El Hamdouni, R., Irigaray, C., Fernandez, T., Chacón, J., & Keller, E. A. (2007). Assessment of relative active tectonics, southwest border of Sierra Nevada (southern Spain). *Geomorphology, 96*, 150–173.

Hack, J. T. (1957). *Studies of longitudinal stream-profiles in Virginia and Maryland*. U.S. Geological Survey Professional Paper 294B, 45–97.

Hack, J. T. (1973). Stream-profiles analysis and stream-gradient index. *Journal of Research of the U.S.*

Geological Survey, 1, 421–429.
Hack, J. T. (1982). *Physiographic division and differential uplift in the piedmont and Blue Ridge*. U.S. Geological Survey Professional Paper 1265, 1–49.
Hare, P. W., & Gardner, T. W. (1985). Geomorphic indicators of vertical neotectonism along converging plate margins, Nicoya Peninsula, Costa Rica. In: *Morisawa, M., Hack, J.T.*
Hessami ,kh., Jamali ,F . & tabassi ,H. (2003). Major Active Faults of Iran ,Map .
Keller, E. A. (1986). Investigation of active tectonics: use of surficial Earth processes. In: *Wallace, R.E. (Ed.). Active tectonics Studies in Geophysics*, National Academy Press, Washington DC, pp. 136–147.
Keller, E., & Pinter, N. (1996). *Active tectonics, Earth quakes, uplift and, Earth sciences series.* prentice-Hall, New Jersey.
Keller, E. A., & Pinter, N. (2002). *Active Tectonics: Earthquakes, Uplift, and Landscape* (2nd Ed.). Prentice Hall, New Jersey.
Mayer, L. (1990). *Introduction to Quantitative Geomorphology*. Prentice Hall, Englewood, Cliffs, NJ.
Molin, P., Pazzaglia, F. J., & Dramis, F. (2004). Geomorphic expression of active tectonics in a rapidly-deforming forearc, sila massif, Calabria, southern Italy. *American Journal of Science 304*, 559–589.
Nabavi, M. H. (1976). *A Preface to Iran's Geology*. 109 p.
Nowroozi, A. A., & Mohajer-Ashjai, A. (1985). Fault movements and tectonics of Eastern Iran: boundaries of the Lut plate. *Geophys. J. R. astr. Soc., 83*, 215-237.
Ramírez-Herrera, M. T. (1998). Geomorphic assessment of active tectonics in the Acambay Graben, Mexican volcanic belt. *Earth Surface Processes and Landforms, 23*, 317–332.
Reddy, G. P. O., Maji, A. K., & Gajbhiye, K. S. (2004). Drainage morphometry and its influence on landform characteristics in a basaltic terrain, Central India a remote sensing and GIS approach. *International Journal of Applied Earth Observation and Geo information, 6*, 1–16.
Rockwell, T. K., Keller, E. A., & Johnson, D. L. (1985). Tectonic geomorphology of alluvial fans and mountain fronts near Ventura, California. In: Morisawa, M. (Ed.), Tectonic Geomorphology, *Proceedings of the 15th Annual Geomorphology Symposium. Allen and Unwin Publishers, Boston*, pp. 183–207.
Silva, P. G., Goy, J. L., Zazo, C., & Bardajm, T. (2003). Fault generated mountain fronts in Southeast Spain: geomorphologic assessment of tectonic and earthquake activity. *Geomorphology, 250*, 203–226.
Troiani, F., & Della Seta, M. (2008). The use of the stream length–gradient index in morphotectonic analysis of small catchments: a case study from Central Italy. *Geomorphology, 102*, 159–168.
Strahler, A. N. (1952). Hypsometric (area–altitude) analysis of erosional topography. *Geological Society of America Bulletin, 63*, 1117–1142.